Supporting Information: Site-specific siderocalin binding to ferric and ferric-free enterobactin as revealed by mass spectrometry

Chunyang Guo[1], Lindsey K. Steinberg[2], Ming Cheng[1], Jong Hee Song[1], Jeffrey P. Henderson[2*], Michael L. Gross[1*]

1. Department of Chemistry, Washington University, St. Louis, Missouri 63130, United States
2. Division of Infectious Diseases, Department of Medicine, the Center for Women's Infectious Disease Research, Washington University School of Medicine, St. Louis, Missouri 63110

Methods

Materials PBS buffer (pH 7.5), water, urea, formic acid, acetimidate hydrochloride, methylgloxal, ammonium acetate, tetrahydrofuran (THF), iron (III) chloride, (tris(2-carboxyethyl)phosphine) hydrochloride (TCEP), iodoacetamide (IAM), thrombin, p-aminobenzamidine agarose, DEAE sepharose, and C18 octadecyl-functionalized silica gel were obtained from Sigma-Aldrich (St. Louis, MO). Trypsin, chymotrypsin, and Glu-C were purchased from Promega (Madison, WI). Zeba™ spin desalting column (7K MWCO) and Pierce glutathione agarose were purchased from Thermo Scientific (Rockford, IL). Sartorius™ Vivaspin™ (5K cutoff) 500 µL concentrators was from Sartorius Corporation (Gottingen, Germany).

Protein and Ligand Purification Human Scn protein was expressed and purified as previously described, (*1)* using the hScn-gst-pGEX4T plasmid kindly gifted to the Henderson lab by Roland Strong. Lin-Ent was chromatographically purified from conditioned media as follows. M63 minimal salts media without $FeSO_4$, supplemented with 0.2% glycerol, 10 µg/mL niacin, 20 uM dipyridyl, and 200 uM 2,3-dihydroxybenzoic acid was inoculated 1:1000 with stationary phase LB culture of the enterobactin producer UTI89ΔybtSΔiroA, and incubated overnight at 37°C. $FeCl_3$ was added to the clarified supernatant (>3mM), until a deep purple color was obtained. Ferric catecholates were purified on a benchtop DEAE column and eluted with 7.5 M acidified ammonium formate. Ferric complexes were reductively dissociated with 120 mM sodium

dithionite and Ent were purified on a benchtop C18 column. Lin-Ent was purified from concentrated eluate by reversed phase HPLC (Supelco Ascentis C18 column, cat#: 581358-U). Fractions containing pure linear enterobactin were confirmed by LC-MS, lyophilized, and stored dry at -20°C. Linear enterobactin was suspended in ethanol + 0.1% formic acid for use, and concentration was measured via UV-vis absorbance spectroscopy with ε_{319nm} = 11,200$M^{-1}cm^{-1}$. (*2,3)*

Preparation of Protein Stock Solution. Scn (100 µM) was prepared in PBS buffer. The (2,3-DHB-^{L}Ser)$_3$-bound Scn was prepared by incubating the ligand (60 µM) with the Scn (40 µM) for 3 h at 25 ^{o}C. The [Fe(2,3-DHB-^{L}Ser)$_3$]$^{3-}$-bound Scn complex was prepared by incubating $FeCl_3$ (72 µM) and lin-Ent (60 µM) for 2 h at room temperature, then equilibrating the mixture with Scn (40 µM) for 4 h at room temperature.

Native Mass Spectrometry. A solution of 100 µM Scn was prepared in 50 mM ammonium acetate buffer. The Scn stock solution was buffer exchanged three times in a Sartorius™ Vivaspin™ concentrator (5K cutoff). Complexes of lin-Ent and ferric lin-Ent-bound Scn were prepared by using the procedure described above. A 5-µL sample was loaded on a nanoES spray capillary interfaced with Exactive Plus EMR (Thermo Scientific, Bremen, Germany) mass spectrometer operating with a *m/z* range from 1000-6000. Orbitrap EMR settings were: 1500 V capillary voltage, 250 ^{o}C capillary temperature, 200 ms injection time. Data were analyzed using Thermo Xcalibur (Thermo Scientific).

H/D exchange (HDX). For mapping, 100 pmol of protein (in 1 µL) was diluted in PBS buffer (24 µL) at 37 ^{o}C for 5 min and quenched by adding 25 µL quench solution (4 M guanidine chloride, 50 mM TCEP in water, 25% (v/v) trifluoroethanol with pH 2.5). After 3 min denaturation at 37^{o}C, the quenched sample was diluted by 1% TFA in water (pH 2.5) to 250 µL and then injected into a custom-fabricated on-line pepsin column. The digested protein sample was trapped on a C8 column and separated on a C18 analytical column.

To initiate exchange, 100 pmol of protein (1 µL) was diluted in deuterated PBS buffer (24 µL) at 37^{o}C. After certain times, from 10 s to 4 h, the exchange was quenched by adding 25 µL of the quench solution mentioned above. The H/D exchange data was collected on an LTQ FT mass spectrometer (Thermo, Waltham, MA). LC elution was performed using a gradient solvent system [solvent A: water with 0.1% formic acid, solvent B: 80% acetonitrile and 20% water with 0.1%

formic acid]. The flow rate was 100 µL/min. Gradient elution was as follows: solvent A delivered at a linear gradient from 95% to 50% for 5.5 min, followed by a linear gradient to 0% in 0.5 min. Solvent B was then maintained at 100% for 1.5 min before column re-equilibration.

Global intact protein analysis. Mass spectra of intact proteins were acquired on Bruker MaXis Q-TOF (Bremen, Germany). Protein sample (50 pmol) was injected to a custom-built platform where the protein was captured by a C8 trap column and desalted at 200 uL/min of H_2O containing 0.1% trifluoracetic acid for 3 min. After the on-line desalting, the protein was eluted with a 8 min gradient of 5% to 80% acetonitrile in 0.1% formic acid at a flow rate of 100 uL/min.

Lysine and Arginine Footprinting. Experiments were performed in triplet by incubating 10 µM protein with 10 mM ETAT or MG. After 1 min, 3 min, 5 min, 10 min of reaction at 37 ^{o}C, the reaction was quenched by removing the reagents by using a Zeba spin desalting column.

Proteolysis Protocol. The filtrate, after desalting, was evaporated to dryness in a vacuum centrifuge. The pellets obtained were resuspended in 50 µL water. An aliquot of 20 µL resuspended solution was denatured at 95 ^{o}C for 30 min, followed by adding 8 M urea, 50 mM TCEP, and 50 mM IAM. For chymotrypsin digestion, proteins were then digested overnight with a protease:protein ratio of 1:20 (w/w) at 37 ^{o}C. For GluC/trypsin co-digestion: proteins were digested with GluC for 8 h at 37 ^{o}C. Trypsin was then added into the solution. The digested sample was kept at 37 ^{o}C overnight. Pure formic acid (1 µL) was added to stop the digestion.

Proteolytic peptides analysis. The experiment was performed on a Q-Exactive Plus hybrid quadrupole orbitrap mass spectrometer coupled with a Nanospray Flex ion source. (Thermo Scientific, Bremen, Germany). A C18 column was custom fabricated and interfaced with an integrated emitter (75 µm × 150 mm, 1.8 µm, 100 Å). The gradient started with 98% solvent A (water with 0.1% formic acid) and 2.0% solvent B (80% acetonitrile, 0.1% formic acid), then linearly increased to 20% solvent B over 55 min, increased to 50% solvent B over 25 min, and finally increased to to 90% solvent B over 10 min followed by a 15 min re-equilibration step. The mass range was set from *m/z* 380-2200 with a mass resolving power of 70 K (at *m/z* 200). The 15 most abundant molecular ions were automatically chosen for fragmentation (DDA). Precursor ions were isolated in the quadrupole with an isolation window of 2.0 *m/z* and fragmented with higher-energy collisional dissociation (HCD) with a normalized collision energy (NCE) of 32% of

maximum. The automatic gain control (AGC) targets were 5×10^5 for MS and 5×10^4 for MS/MS acquisitions. Maximum injection times (maxIT) were 200 ms for MS and 100 ms for MS/MS.

Data analysis. For HDX data, the peptide identification was accomplished through a combination of accurate mass analysis and LC-MS/MS using Protein Metrics (San Carlos, CA). The following parameters were applied: nonspecific for the digestion specificity, while allowing for up to 2 missed cleavages, 60 ppm precursor mass tolerance, and 0.5 Dalton fragment mass tolerance. Raw data were manually checked, and the list of verified peptides were submitted to HDX Workbench (Honolulu, HI) in an automated way. Deuterium uptake was calculated as previously described. *(4)* The deuterium uptake % can be calculated using the equation 1, where $m_{0\%}$ is the centroid mass of non-deuterated peptide, and $m_{100\%}$ is the centroid mass of fully deuterated peptide, and m is the centroid of the observed peptide.

$$D = \frac{m - m_{0\%}}{m_{100\%} - m_{0\%}} \qquad \text{Equ 1}$$

For differential HDX experiments, the LC-MS/MS data were searched for unmodified and modified Scn digested peptides by using Byonic Software (Protein Metrics, San Carlos, CA). All MG and ETAT modifications on Arg and Lys were added as modifications to the database. The parameters were: 10 ppm precursor mass tolerance, 60 ppm fragment mass tolerance. The modifications on each residue were verified by manually checking the product-ion (MS/MS) spectra.

Figure S1. HDX mapping showing 87% coverage with denaturation of the protein by 4 M guanidine quench buffer.

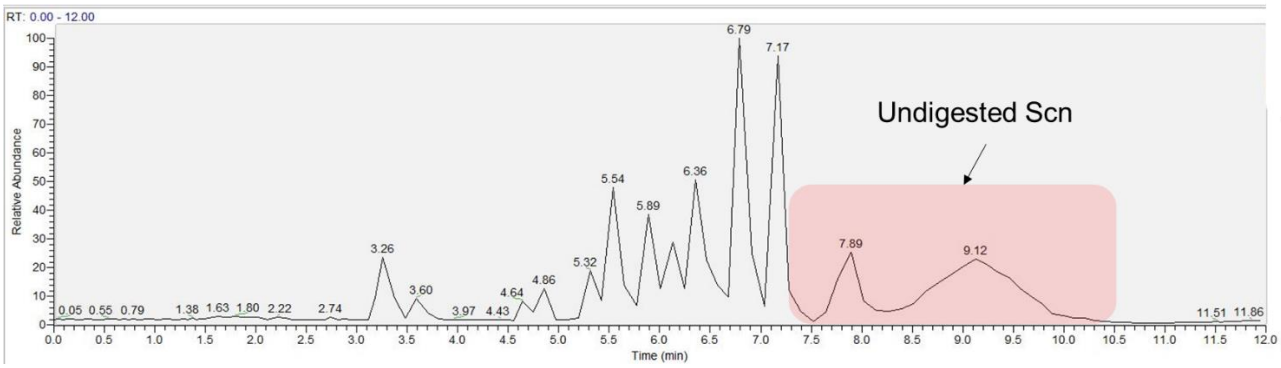

Figure S2. Full chromatogram of the HDX mapping with 4 M guanidine quench buffer.

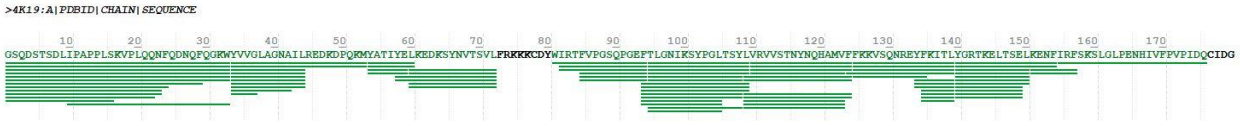

Figure S3. HDX mapping showing 93% coverage with denaturation of the protein by 4 M guanidine and 50% trifluoroethanol quench buffer.

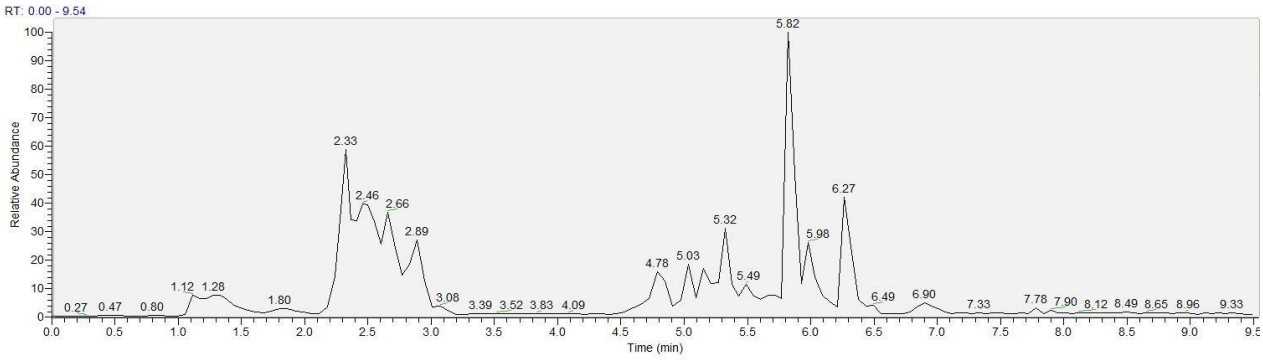

Figure S4. Full chromatogram of the HDX mapping with 4 M guanidine and 50% trifluoroethanol quench buffer.

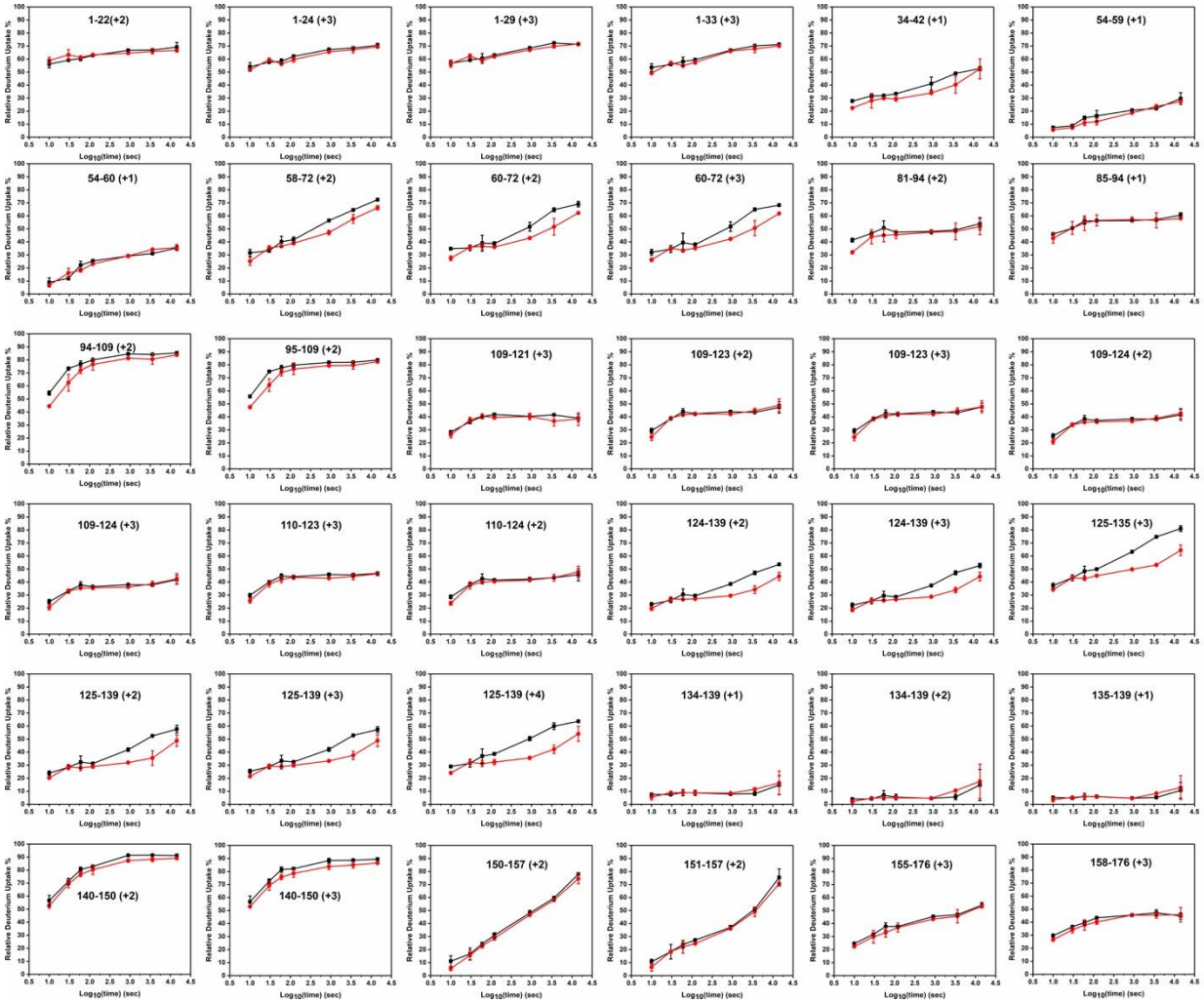

Figure S5. HDX kinetic plots of peptides from Scn (black) and aferric lin-Ent-bound Scn (red).

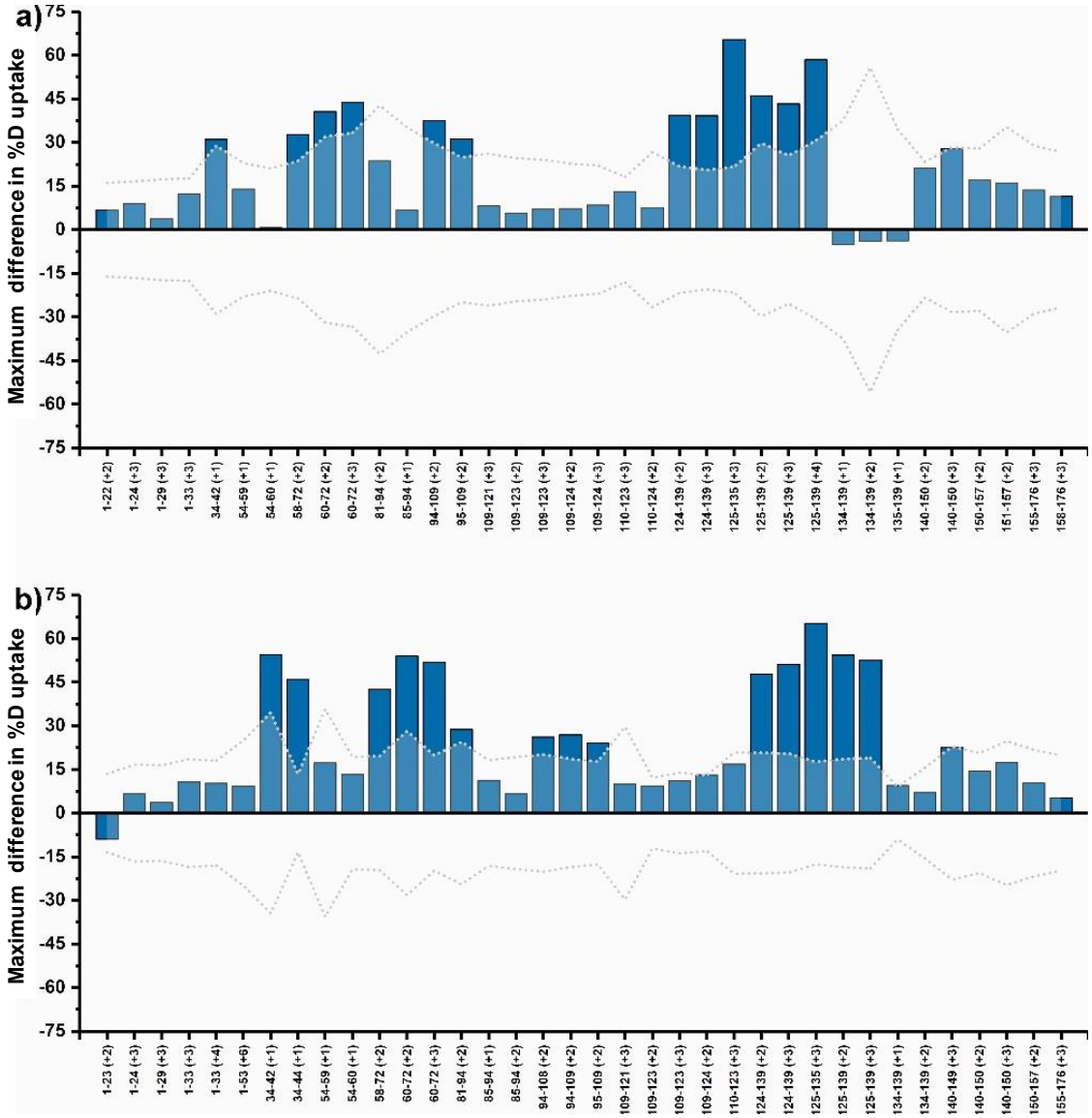

Figure S6. The cumulative changes in HDX rates. Blue bars represent the difference in percent deuterium uptake between the complexed and non-complexed SCN protein. a) (% deuterium uptake of Scn - % deuterium uptake of lin-Ent bound Scn), and b) (% deuterium uptake of Scn - % deuterium uptake of ferric lin-Ent bound Scn). The propagation error for each peptide is equal to the square root of the sum of all squared standard deviation values for the collective measurement of (% deuterium uptake of apo - % deuterium uptake of holo). Three times of propagation error of each peptide is depicted in grey. HDX was considered to be significantly different between the bound and apo forms if the difference in percent deuterium uptake (blue bars) was greater than three times the propagations error (grey).

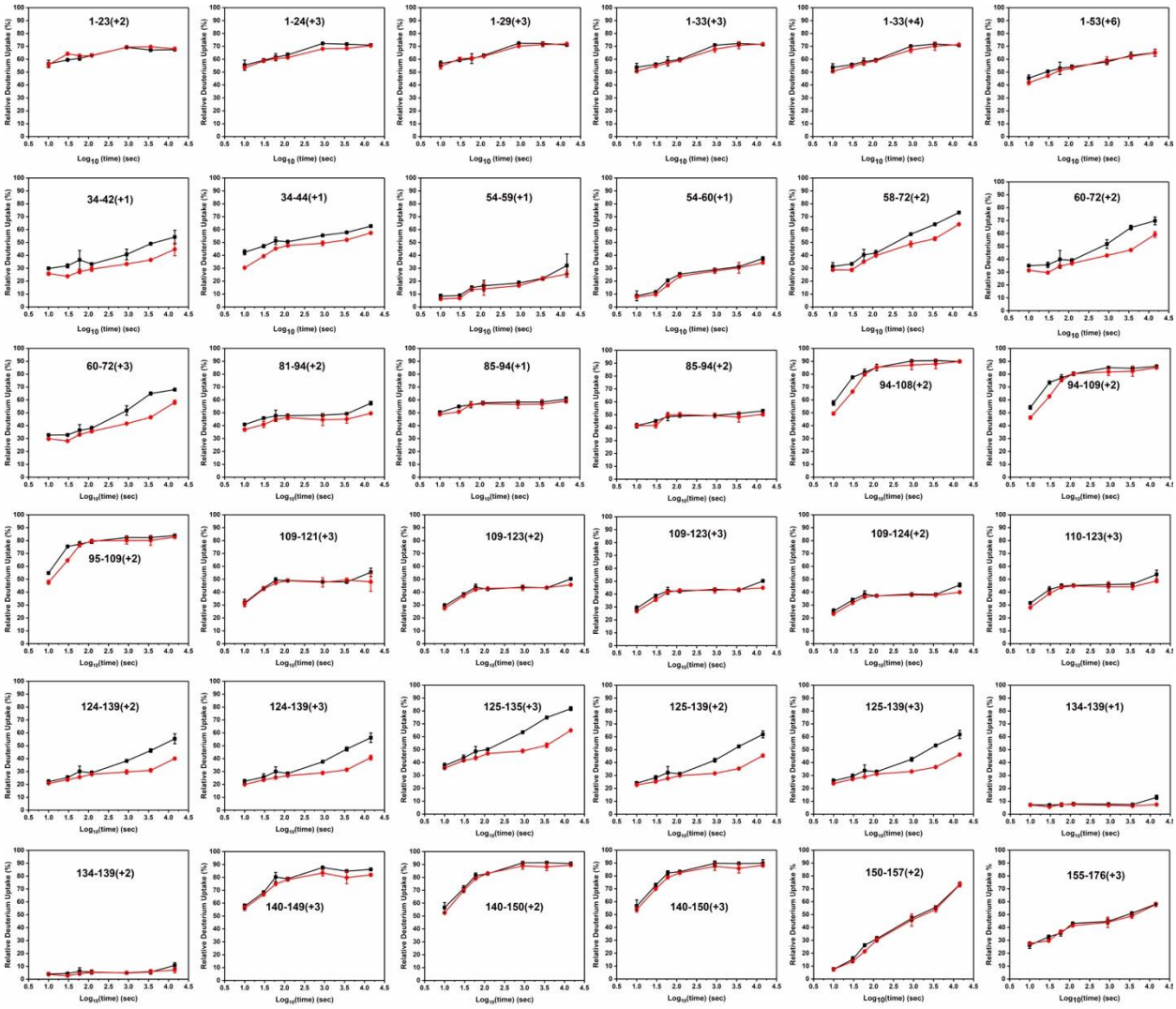

Figure S7. HDX kinetic plots of peptides from Scn (black) and ferric lin-Ent-bound Scn (red).

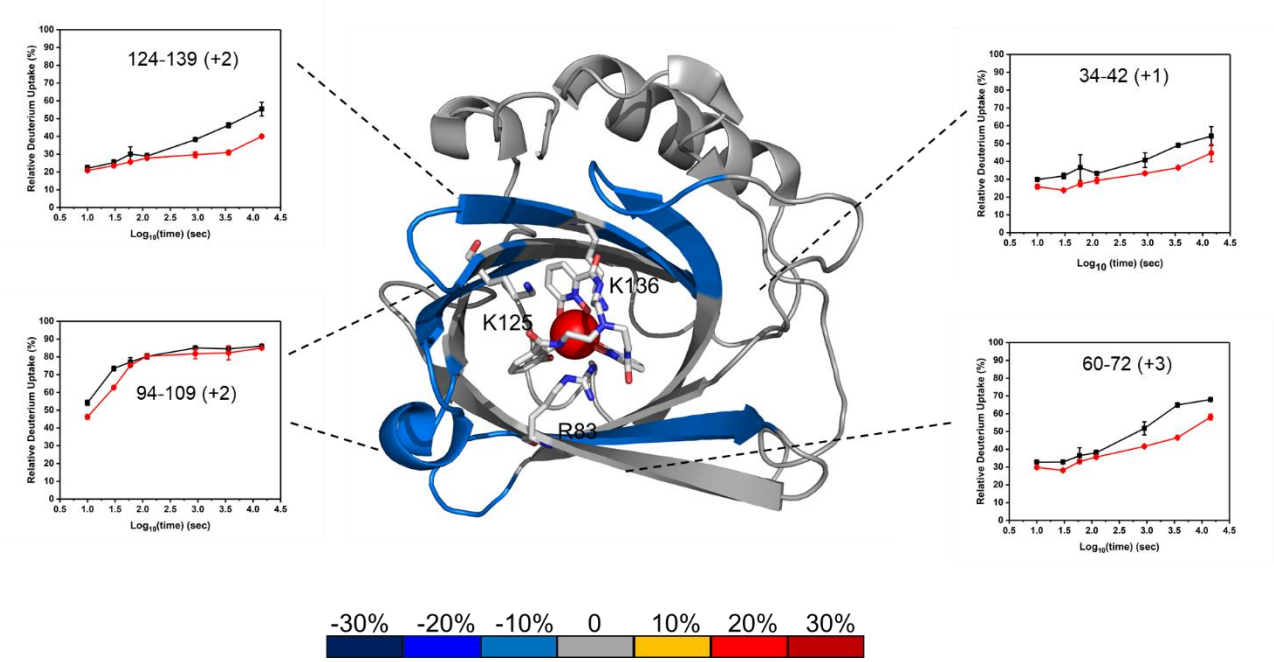

Figure S8. Structure: Average percentage differences in deuterium uptake between apo-Scn and ferric lin-Ent-bound Scn color-indicated on an X-ray crystal structure of TrenCam-bound Scn (PDB 3HWG). Insets: HDX data for select peptides in the bound and unbound state. Apo-Scn (black) and ferric lin-Ent-bound Scn (red).

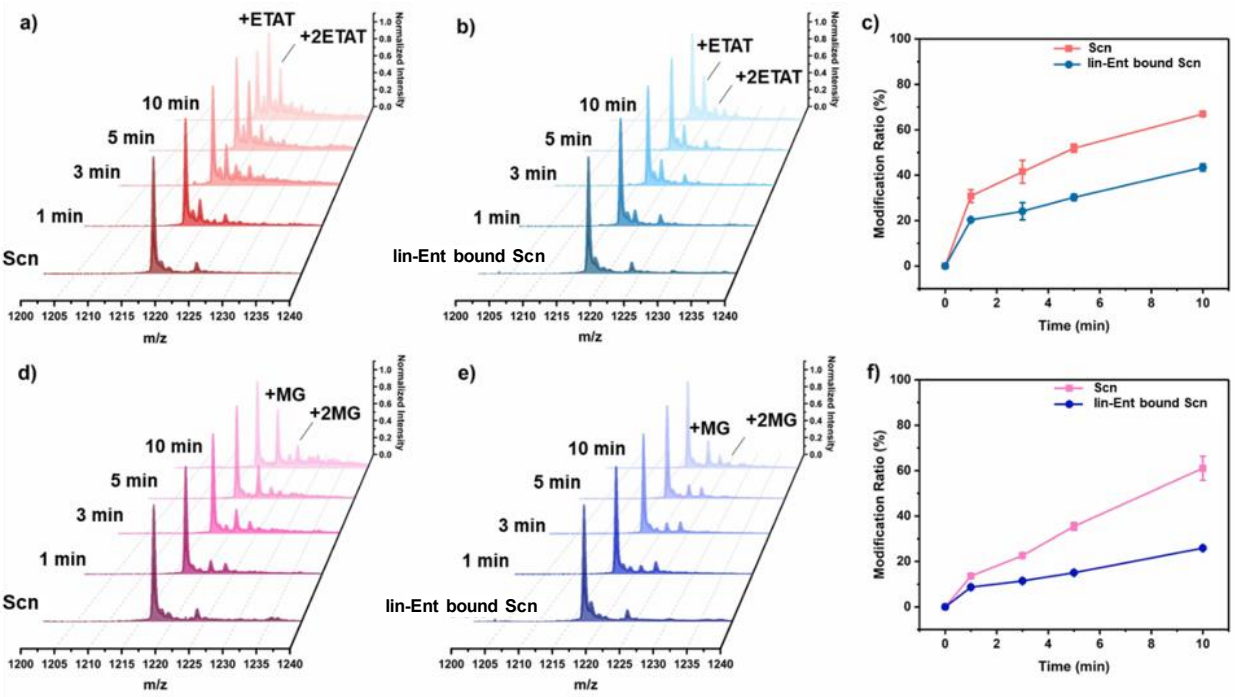

Figure S9. Mass spectra of the intact, unbound Scn (**a**) and aferric lin-Ent-bound Scn (**b**) as a function of ETAT footprinting time. **(c)** Plot of the time-dependent ETAT modification ratio. Mass spectra of intact, unbound Scn (**d**) and aferric lin-Ent-bound Scn (**e**), as a function of MG footprinting time. (**f**) Plot of the time-dependent MG modification ratio.

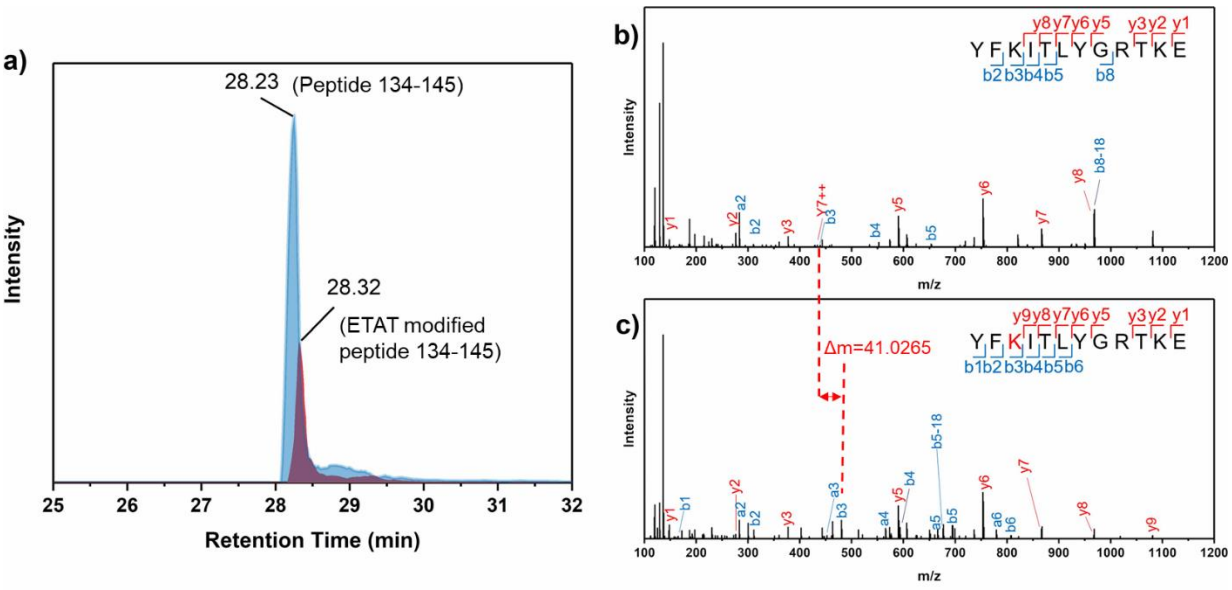

Figure S10. Chromatograms (**a**) and product-ion (MS/MS) spectra of (**b)** unlabeled, and (**c)** ETAT labeled representative peptide 134-145 with +3 charge state. K136 can become ETAT modified.

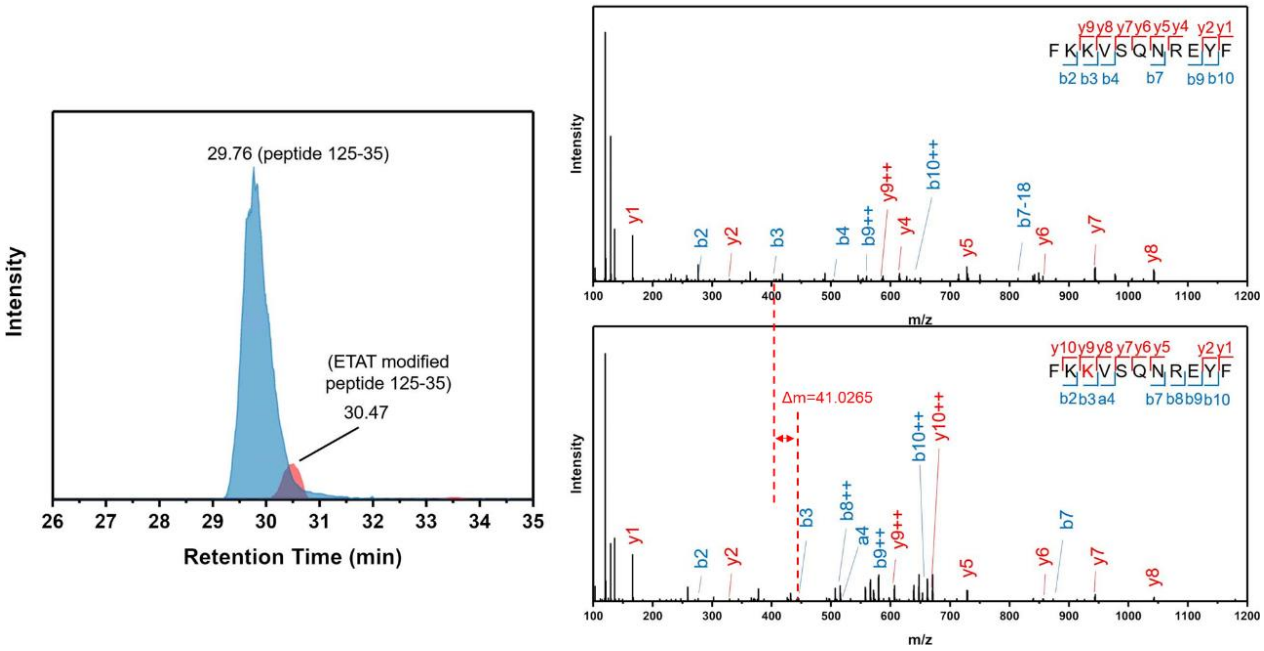

Figure S11. Chromatograms (**a**) and product-ion (MS/MS) spectra of (**b)** unlabeled, and (**c)** ETAT labeled representative peptide 125-135 with +3 charge state. K127 can become ETAT modified.

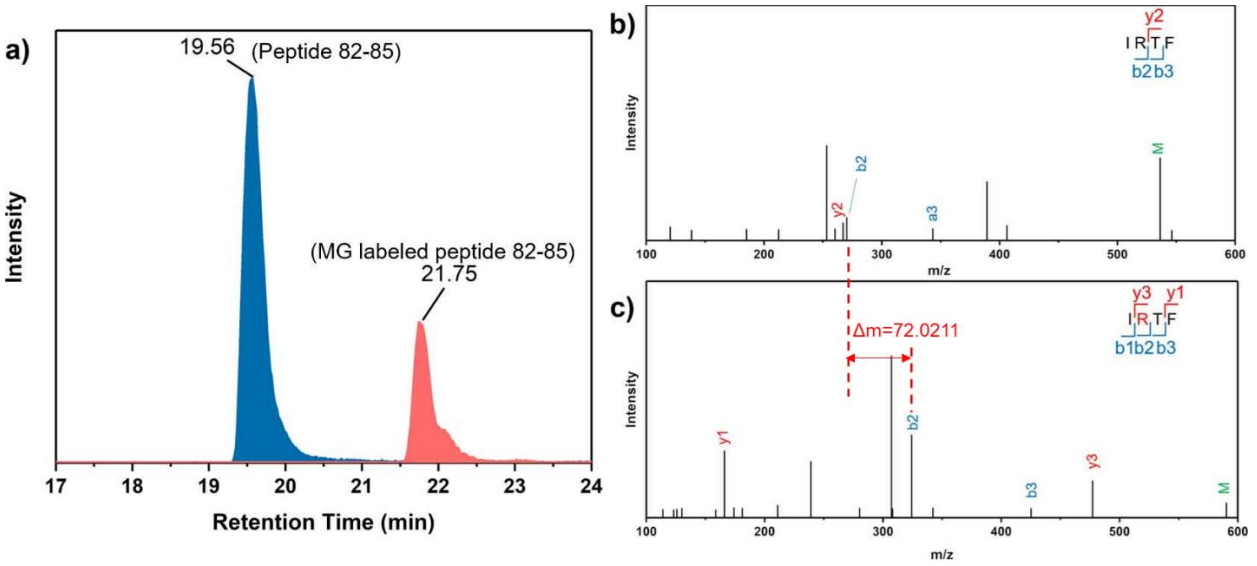

Figure S12. Chromatograms (**a**) and product-ion (MS/MS) spectra of (**b)** unlabeled, and (**c)** MG labeled representative peptide 82-85 with +1 charge state. R83 can become MG modified.

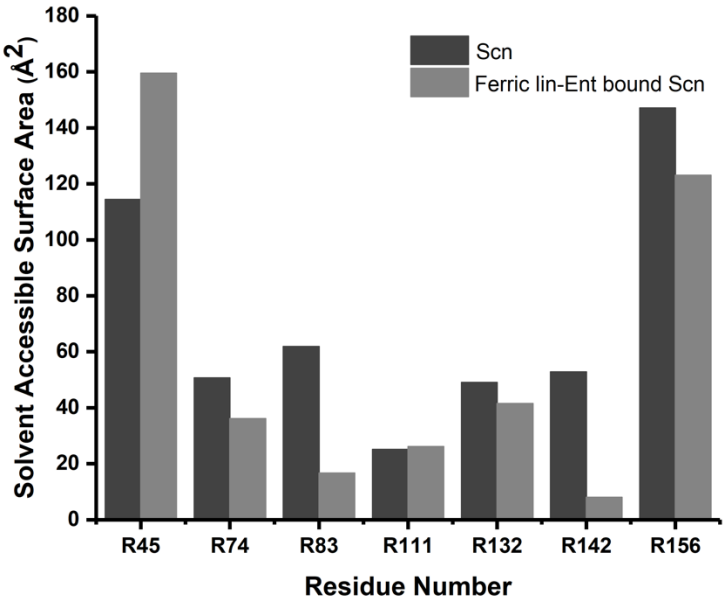

Figure S13. Comparison of solvent accessible surface area (SASA) calculated in PyMol between Scn and ferric lin-Ent bound Scn.

Table S1 Summary of the ETAT modification % for different peptide regions in apo-Scn, lin-Ent-bound Scn, and ferric lin-Ent-bound Scn. (The region represented by a peptide is considered to undergo large conformational change when the *p* values are less than 0.01. (a) represents the difference between unbound Scn and lin-Ent bound Scn, (b) represents the difference between unbound Scn and Fe-lin-Ent bound Scn.)

Residue Number	ETAT Modification (%)			Modification extent difference (a)	*P* value (a)	Modification extent difference (b)	*P* value (b)
	Scn	lin-Ent Scn	Fe-lin-Ent Scn				
K17	3.88×10^{-1}	2.70×10^{-1}	3.85×10^{-1}	3.04×10^{-1}	8.77×10^{-3}	7.74×10^{-3}	9.49×10^{-1}
K32	4.31	5.65	7.71	-3.11×10^{-1}	1.14×10^{-1}	-7.91×10^{-1}	1.33×10^{-1}
K48	1.6×10^{-1}	1.47×10^{-1}	1.65×10^{-1}	8.44×10^{-2}	1.94×10^{-2}	-3.12×10^{-2}	3.15×10^{-2}
K52	2.04	2.23	1.72	-9.18×10^{-2}	4.15×10^{-1}	1.56×10^{-1}	1.53×10^{-1}
K64	12.7	18.7	16.6	-4.74×10^{-1}	5.64×10^{-1}	-3.12×10^{-1}	6.28×10^{-1}
K100	4.81	3.84	5.12	2.02×10^{-1}	1.66×10^{-1}	-6.47×10^{-2}	5.16×10^{-1}
K126	2.77	2.69	2.23	2.63×10^{-2}	4.85×10^{-1}	1.94×10^{-1}	1.26×10^{-1}
K127	20.3	6.23	6.04	6.92×10^{-1}	3.81×10^{-4}	7.02×10^{-1}	5.57×10^{-4}
K136	12.7	1.91	2.28	8.50×10^{-1}	3.36×10^{-4}	8.20×10^{-1}	2.29×10^{-4}
K151	4.43×10^{-1}	4.56×10^{-1}	5.15×10^{-1}	-3.10×10^{-2}	4.55×10^{-1}	-1.63×10^{-1}	1.28×10^{-1}
K159	33.4	32.0	38.8	-4.14×10^{-2}	5.06×10^{-1}	-1.62×10^{-1}	6.92×10^{-2}

Table S2 Summary of the MG modification % for different peptide regions in apo-Scn, lin-Ent-bound Scn, and ferric lin-Ent-bound Scn. (The region represented by a peptide is considered to undergo large conformational change when the *p* value is less than 0.01. (a) represents the difference between unbound Scn and lin-Ent bound Scn, (b) represents the difference between unbound Scn and Fe-lin-Ent bound Scn.)

	MG Modification (%)						
Residue Number	Scn	lin-Ent bound Scn	Fe-lin-Ent bound Scn	Modification extent difference (a)	*P* value (a)	Modification extent difference (b)	*P* value (b)
R45	17.9	16.4	16.8	8.03×10^{-2}	7.2×10^{-1}	5.94×10^{-2}	8.38×10^{-1}
R74	16.7	7.0	9.45	5.83×10^{-1}	9.43×10^{-2}	4.33×10^{-1}	1.54×10^{-1}
R83	31.1	5.18	6.46	8.33×10^{-1}	5.91×10^{-3}	7.92×10^{-1}	4.85×10^{-3}
R111	5.65	6.36	9.328	-1.27×10^{-1}	4.78×10^{-1}	-6.52×10^{-1}	1.89×10^{-2}
R132	26.05	11.6	13.4	5.56×10^{-1}	1.08×10^{-1}	4.88×10^{-1}	9.81×10^{-2}
R142	2.60	0.442	0.366	8.30×10^{-1}	9.90×10^{-2}	8.59×10^{-1}	9.39×10^{-2}
R156	45.6	43.5	36.4	4.75×10^{-1}	4.66×10^{-2}	2.02×10^{-1}	1.66×10^{-1}

References

(1) Shields-Cutler, R. R., Crowley,J. R., Hung, C. S., Stapleton , A. E., Aldrich, C. C., Marschall, J., Henderson, J. P. (2015) Human urinary composition controls antibacterial activity of siderocalin. *J. Biol. Chem. 290*, 15949-15960.

(2) Adler, C., Corbalán, N. S., Seyedsayamdost, M. R., Pomares, M. F., Cristóbal, R. E., Clardy, J., Kolter, R., Vincent, P. A. (2012) Catecholate siderophores protect bacteria from pyochelin toxicity. *PLOS ONE 7*, e46754.

(3) Matzanke, B. F., Ecker, D. J., Yang, T. S., Huynh, B. H., Müller, G., Raymond, K. N. (1986) Escherichia coli iron enterobactin uptake monitored by Mössbauer spectroscopy. *J. Bacteriol. 167*, 674-680.

(4) Masson, G. R., Burke, J. E., Ahn, N. G., Anand, G. S., Borchers, C., Brier, S., Bou-Assaf, G. M., Engen, G. R., Englander, S. W., Faber, J., Garlish, R., Griffin, P. R., Gross, M. L., Guttman, M., Hamuro, Y., Heck, A. J. R., Houde, D., Iacob , R. E., Jørgensen, T. J. D., Kaltashov, I. A., Klinman, J. P., Konermann, L., Man, P., Mayne, L., Pascal, B. D., Reichmann, D., Skehel, M. Snijder, J., Strutzenberg, T. S., Underbakke, E. S., Wagner, C., Wales, T. E., Walters, B. T., Weis, D. D., Wilson, D. J., Wintrode, P. L., Zhang, Z., Zheng, J., Schriemer, D. C., Rand, K. D. (2019) Recommendations for performing, interpreting and reporting hydrogen deuterium exchange mass spectrometry (HDX-MS) experiments. *Nat. Methods*, *16*, 595-602.